AD-A235 730

Annual Report
October 1989 — November 1990
Office of Naval Research
Contract Number N0001490WX24009

Effect of Ripple Load on Stress-Corrosion Cracking in Structural Steels

P.S. PAO AND R.A. BAYLES

Physical Metallurgy Branch
Materials Science and Technology Division
Naval Research Laboratory
Washington, DC 20375-5000

DTIC
ELECTE
MAY 23 1991
S B D

91-00302

Approved for public release; distribution unlimited.

91 5 21 078

REPORT DOCUMENTATION PAGE

Form Approved
OMB No 0704-0188

Public reporting burden for this collection of information is estimated to average 1 hour per response, including the time for reviewing instructions, searching existing data sources, gathering and maintaining the data needed, and completing and reviewing the collection of information. Send comments regarding this burden estimate or any other aspect of this collection of information, including suggestions for reducing this burden to Washington Headquarters Services, Directorate for Information Operations and Reports, 1215 Jefferson Davis Highway, Suite 1204, Arlington, VA 22202-4302, and to the Office of Management and Budget, Paperwork Reduction Project (0704-0188), Washington, DC 20503

1. AGENCY USE ONLY (Leave blank)	2. REPORT DATE	3. REPORT TYPE AND DATES COVERED
	February 1991	

4. TITLE AND SUBTITLE

Effect of Ripple Load on Stress-Corrosion Cracking in Structural Steels

5. FUNDING NUMBERS

6. AUTHOR(S)

Pao, P.S. and Bayles, R.A.

7. PERFORMING ORGANIZATION NAME(S) AND ADDRESS(ES)

Naval Research Laboratory
Code 6326
Washington, DC 20375-5000

8. PERFORMING ORGANIZATION REPORT NUMBER

NRL Publication 190-6320

9. SPONSORING / MONITORING AGENCY NAME(S) AND ADDRESS(ES)

Office of Naval Research
800 N. Quincy Street
Arlington, VA 22217-5000

10. SPONSORING / MONITORING AGENCY REPORT NUMBER

11. SUPPLEMENTARY NOTES

12a. DISTRIBUTION / AVAILABILITY STATEMENT

Approved for public release, distribution unlimited.

12b. DISTRIBUTION CODE

13. ABSTRACT *(Maximum 200 words)*

The presence of small ripple loading can, under certain circumstances, significantly reduce time-to-failure and threshold stress intensity for stress-corrosion cracking (SCC) of steels. A predictive framework for such ripple-loading effects (RLE) is developed from concepts and descriptors used in SCC and corrosion fatigue characterization. The proposed framework is capable of defining critical conditions required for the occurrence of RLE and predicting time-to-failure curves. The agreement between the predicted and laboratory data is excellent.

14. SUBJECT TERMS			15. NUMBER OF PAGES
			16. PRICE CODE
17. SECURITY CLASSIFICATION OF REPORT	18. SECURITY CLASSIFICATION OF THIS PAGE	19. SECURITY CLASSIFICATION OF ABSTRACT	20. LIMITATION OF ABSTRACT
UNCLASSIFIED	UNCLASSIFIED		

NSN 7540-01-280-5500

Standard Form 298 (Rev. 2-89)
Prescribed by ANSI Std. Z39-18
298-102

CONTENTS

DTIC COPY INSPECTED 4

Accession For
NTIS GRA&I ☑
DTIC TAB ☐
Unannounced ☐
Justification
By
Distribution/
Availability Codes
Dist | Avail and/or Special
A-1

EFFECT OF RIPPLE LOAD ON STRESS-CORROSION CRACKING IN STRUCTURAL STEELS

INTRODUCTION

Stress-corrosion cracking (SCC) is a cracking process caused by the conjoint action of stress and a corrodent [1]. Conceptually, SCC will occur if a sensitive material is exposed to a corrosive environment under sufficient stress for a sufficient length of time. For a structural material which contains a crack or crack-like defect, the resistance to SCC is normally evaluated in terms of the fracture mechanics parameter, K_{Iscc}, the threshold stress-intensity factor below which crack extension will not occur. The measurement of K_{Iscc} and its application to design of structures for the marine environment commonly presumes sustained or constant load conditions. Applications in the real world, however - including many in offshore platform structures, rarely involve an absolutely constant load condition, but are far more apt to involve the superposition of relatively small amplitude load perturbations or "ripple load" *. Recent work [3-9] has demonstrated that under such ripple-loading conditions, fracture can occur in some cases at stress-intensity levels much less than K_{Iscc}. Thus, the implications of the ripple-load effect (RLE) may be quite serious. An extensive literature survey on ripple-load effects was recently prepared, which cited several examples from both low- and high-strength and ferrous and nonferrous alloy systems [10].

The objective of this paper is to develop the understanding of the RLE and the framework required for the prediction of the RLE. First of all, the RLE is investigated in two different classes of steels: the medium strength, high toughness 5Ni-Cr-Mo-V steel and the high strength, low toughness AISI 4340 steel. Secondly, the critical conditions required for a material to exhibit RLE in the marine environment are defined and quantitative prediction of the maximum extent of degradation by the RLE is presented. And finally, the quantitative predictive methodology for time-to-failure curves associated with the ripple-load cracking is offered for a given combination of material and loading conditions.

---

*In the context of a "ripple" or small amplitude cyclic load, the stress ratio [2] is generally presumed to be $R \geq 0.90$, although such a stipulation does not affect the generality of the treatment offered in this paper. With regard to notation, the superscript "RL" will be used to denote ripple loading, and the superscript "th" to denote threshold.

MATERIALS AND EXPERIMENTAL PROCEDURES

Two steels studied in this investigation are 5Ni-Cr-Mo-V and AISI 4340 rolled plate materials. Results of chemical analysis and tensile properties are given in Tables 1 and 2, respectively. Time-to-failure data under SCC and RLE conditions were determined using precracked cantilever-beam specimens of length L=400 mm, width W=50.8 mm and thickness B=25.4 mm, with an initial (normalized) crack length of a/W=0.5 and sidegrooves of depth 1.25 mm per side. All tests were conducted in quiescent 3.5% aqueous NaCl solution at ambient temperature. For ripple load cracking, the frequency of the ripple loading was 0.10 Hz (6 cpm), with a skewed triangular load-time waveform having a nine second rise time and a one second fall. Electrode potentials were monitored using a Ag/AgCl reference electrode. The 4340 steel was tested at the freely corroding potential. The 5Ni-Cr-Mo-V steel was tested at a potential of approximately -1.0 V obtained by coupling to zinc anodes. Further procedural details are available elsewhere [5,11].

TABLE I - CHEMICAL COMPOSITIONS (Weight percent)

Material	C	Mn	P	S	Si	Cu	Ni	Cr	Mo	V
5Ni-Cr-Mo-V	0.13	0.82	–	0.002	0.24	0.05	5.20	0.44	0.52	0.05
4340	0.14	0.74	0.01	0.016	0.21	–	2.0	0.74	0.26	0.05

TABLE II - TENSILE PROPERTIES

Material	0.2% Yield Strength, MPa (ksi)	Ultimate Tensile Strength, MPa (ksi)	Elongation in 2-in., %	Reduction in Area, %
5Ni-Cr-Mo-V	965 (140)	1,014 (147)	–	–
4340	1,207 (175)	1,282 (186)	25	11

RESULTS

Ripple-Load Cracking

Ripple-load cracking and SCC experimental results obtained on the 5Ni-Cr-Mo-V and 4340 steels are shown in Figs. 1 and 2. For tests involving ripple-loading, initial K_I corresponds to the maximum stress intensity factor in the loading cycle, as shown in Fig. 3a.

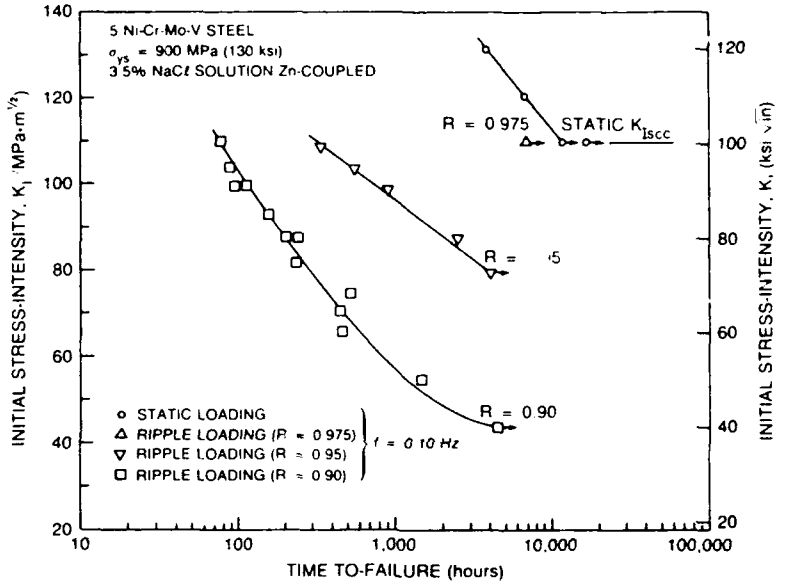

Fig. 1 — Initial stress-intensity (K_I) versus time-to-failure data for 5Ni-Cr-Mo-V steel under static loading and ripple-loading [5].

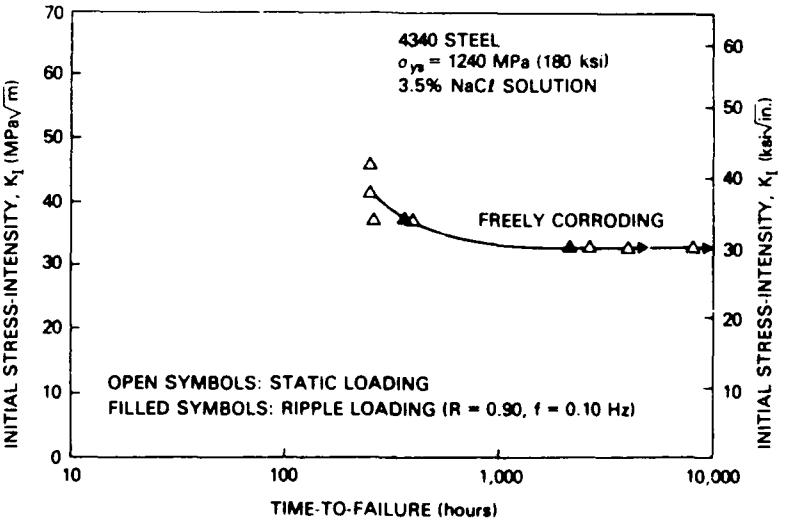

Fig. 2 — Initial stress-intensity (K_I) versus time-to-failure data for high strength 4340 steel under static loading and ripple-loading [5].

For the 5Ni-Cr-Mo-V steel, a static K_{Iscc} was established at 110 MPa $\sqrt{m}$ (100 ksi $\sqrt{in.}$) based upon multiple long-term tests exceeding 10,000 hours. Ripple-loading data were obtained at R values of 0.90, 0.95 and 0.975. Except for R = 0.975, all ripple-loading conditions resulted in reduced values of time-to-failure and lower apparent threshold values. That is, 5Ni-Cr-Mo-V steel is susceptible to RLE under a 5% ripple (R=0.95) and a 10% ripple (R=0.90) conditions. For R = 0.975, the apparent threshold equaled the static K_{Iscc}. For R = 0.95 and 0.90, the apparent thresholds were 80 and 44 MPa$\sqrt{m}$ (74 and 40 ksi$\sqrt{in.}$), respectively. As we will see in the upcoming analysis, these thresholds estimated from 4000-hour exposures are indeed nonconservative.

For the 4340 steel, a long-term static K_{Iscc} value was established at 33 MPa$\sqrt{m}$ (30 ksi$\sqrt{in.}$) [5]. Superimposed on these K_I vs. time-to-failure data curve are two ripple-loading tests with R = 0.90 (largest ripple). As shown in Fig. 2, no effect of ripple-loding on time-to-failure was observed in the 4340 steel. In other words, 4340 steel is not susceptible to RLE even with a 10% ripple (R = 0.90).

Analysis of Ripple-Load Effect

In this paper, ripple-load cracking is approached as an extreme case of corrosion-fatigue crack growth behavior. The desired predictive framework for RLE necessarily involves the interface between SCC and corrosion-fatigue behavior. Thus, the analysis begins with consideration of the relationship between the small amplitude stress-intensity range associated with ripple loading, ΔK, the threshold for corrosion fatigue, ΔK_{th}, K_{max}, and K_{Iscc}.

A. Critical Conditions (for susceptibility)

To define the critical conditions required for a material to exhibit the RLE in marine environment, consider first of all the nature of the interface between stress-corrosion cracking and corrosion fatigue, as represented in the schematics of Fig. 3. In Fig. 3b, the SCC resistance is indicated by the "static" loading curve, wherein the level of K represents the initial value of stress-intensity factor associated with a precracked

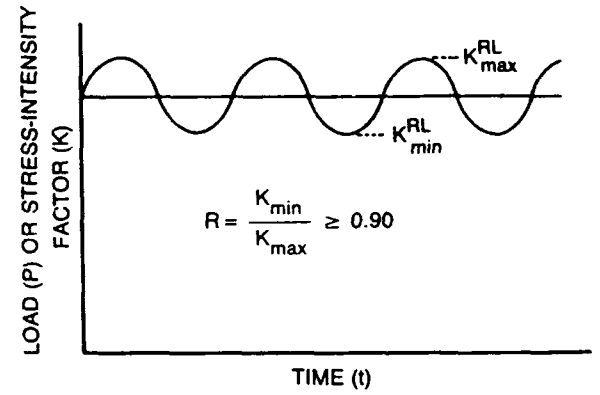

(a)

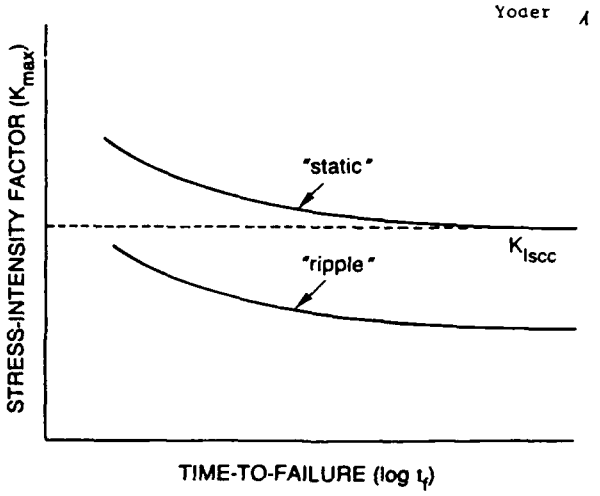

(b)

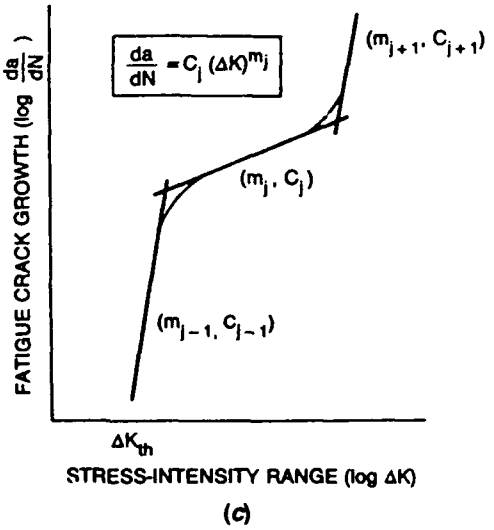

(c)

Fig. 3 — Schematics on analysis of RLE. (a) "ripple" or small amplitude cyclic load superposed on much larger sustained load; stress ratio, $R \geq 0.90$. (b) ripple-load degradation analyzed via K_{max} parameter versus "static" K_{Iscc} threshold; cf. text. (c) piecewise analysis of corrosion-fatigue crack growth rate curve via power-law approximation to j^{th} segment.

specimen (or structure) which is subjected to a constant load. However, if this constant load is superposed with a "ripple" or small-amplitude cyclic load --- as in the schematic of Fig. 3a, then, for a material exhibiting susceptibility to the RLE, cracking resistance appears to be degraded to levels significantly below the "static" threshold K_{Iscc}, as in Fig. 3b. There, the K-level plotted for the "ripple" curve is actually K^{RL}_{max}, the maximum level of K in the ripple-load cycle, cf. Fig. 3a. If RLE is defined as degradation relative to the "static" K_{Iscc} threshold, then the first condition for the RLE can be expressed as:

$$K^{RL}_{max} \leq K_{Iscc} \tag{1}$$

With the treatment of ripple-load cracking as an extreme case of very high stress ratio corrosion fatigue crack growth, then with reference to Fig. 3a, this condition can be represented in terms of stress-intensity range [2],

$$\Delta K^{RL} \leq (1-R)\ K_{Iscc} \tag{1a}$$

Now the resistance of a material to corrosion fatigue crack growth is normally reported in terms of fatigue crack growth rate (da/dN) as a function of ΔK, as shown in Fig. 3c. The lower limit of the ΔK spectrum is defined by ΔK_{th}, the threshold level below which cracks will not propagate (while the upper bound is controlled by the fracture toughness). Consequently, cracks cannot propagate to failure under ripple-loading for any material unless this second condition is also met:

$$\Delta K^{RL} \geq \Delta K_{th} \tag{2}$$

Or, equivalently, the threshold level of K --- below which ripple-load cracking will not occur, is given by:

$$K^{RL}_{max}\,|_{th} = \frac{\Delta K_{th}}{1-R} \tag{2a}$$

Consequently, if conditions (1) and (2) are combined, it can be stated that a material will exhibit a susceptibility to the RLE if and only if:

$$\frac{\Delta K_{th}}{1-R} \leq K_{max}^{RL} \leq K_{Iscc} \qquad (3)$$

Or, equivalently,

$$\Delta K_{th} \leq \Delta K^{RL} \leq (1-R)\ K_{Iscc} \qquad (3a)$$

B. Maximum Extent of Degradation

Relation (3) thus defines a "window" for which the RLE would be anticipated --- as sketched in Fig. 4a. If one considers the differential between the threshold for ripple-load cracking $\left(K_{max}^{RL}\,|_{th}\right)$ and K_{Iscc}, then the maximum amount of degradation attributable to the RLE is given by:

$$\%\ \text{degradation}\,|^{RL} = \left[1 - \frac{\Delta K_{th}}{K_{Iscc}\,(1-R)}\right] 100 \qquad (4)$$

On the other hand, if conditions of relation (3) are not met, a material will not exhibit susceptibility to the RLE --- as illustrated in Fig. 4b, since**

$$\frac{\Delta K_{th}}{1-R} > K_{Iscc} \qquad (5)$$

C. Quantitative Prediction of Time-to-Failure (t_f) Curves

**This statement and the preceding are contingent, of course, upon definition of the RLE as degradation relative to the K_{Iscc} threshold. If however, attention were to be focused on cracking behavior above K_{Iscc}, then it is important to recognize that for levels of K_{max} in excess of K_{Iscc} in the "susceptible" case --- or in excess of $K_{max}^{RL}\,|_{th}$ in the "nonsusceptible" case, "ripple" or cyclic loading at R≥0.90 will definitely affect the time-to-failure (t_f). For a given geometry, reduction in tf would be anticipated from levels associated with "static" loading, in accord with the superposition model of corrosion fatigue [12]. These reduced levels of t_f can still be computed using the framework described in the following section.

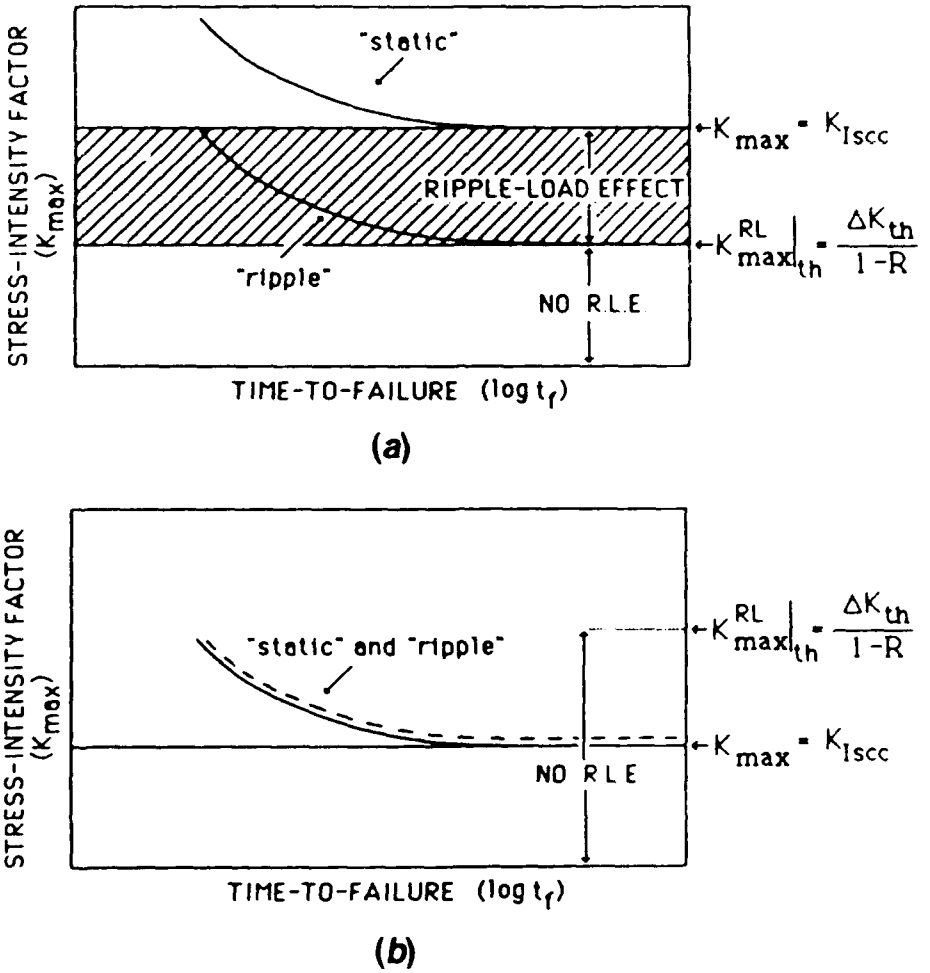

Fig. 4 — Illustration of predictions from relation (3); cf. text. (a) susceptibility to RLE. (b) non-susceptibility to ripple-load degradation.

Though the typical logarithmic corrosion-fatigue crack-growth rate curve may well exhibit a more complex shape than shown in the schematic of Fig. 3c, nevertheless, it can be approximated in piecewise fashion with power-law segments,

$$\frac{da}{dN} = C_j(\Delta K)^{m_j} \qquad (6)$$

(Of course, there are many other appropriate means to analytically characterize fatigue crack growth behavior - e.g. as suggested in the elegant treatment of Krausz and Krausz [13].)

Thus, the total number of cycles to propagate a crack to failure follows the piecewise integration (over j segments) as [2]:

$$(N_p)_j = \int_{(a_i)_j}^{(a_f)_j} \frac{da}{C_j\left[(1-R)\ P_{max}\ f(a,Q)\right]^{m_j}} \qquad (7)$$

where P is load and $f(a,Q)$ is a function of crack length (a) and structural geometry (Q). Since time-to-failure is simply given by:

$$t_f = \frac{\sum_j (N_p)_j}{\nu} \qquad (8)$$

where ν is the cyclic frequency, then t_f can be estimated as:

$$t_f = \frac{1}{\nu} \sum_j \int_{(a_i)_j}^{(a_f)_j} \frac{da}{C_j\left[(1-R)\ P_{max}\ f(a,Q)\right]^{m_j}} \qquad (9)$$

Though in certain cases f(a,Q) is sufficiently simple to permit direct integration of Eq. 9 --- such as in the case of a center-cracked tension panel, in general, a numerical integration will facilitate computation.

D. Tests of the Predictive Framework

Of the two materials studied in this investigation, 5Ni-Cr-Mo-V steel and 4340 steel, the former is highly susceptible to RLE while the latter is not. As we shall see later, characteristics of both can be predicted from the proposed framework.

i) 5Ni-Cr-Mo-V Steel

As shown in Fig. 1, ripple-loading has a strongly deleterious effect in 5Ni-Cr-Mo-V steel on both apparent threshold levels and on time-to-failure [5]. The apparent threshold levels and time-to-failure under ripple-loading conditions can be analytically predicted from Eqs. 2 and 9, provided that the threshold stress intensity range and the corrosion fatigue crack-growth rate corresponding to the particular stress ratio in a similar environment can be established. Vosikovsky has conducted a systematic investigation on the effect of stress ratio on the fatigue crack growth rate in 3.5% NaCl solution on a 5Ni-Cr-Mo-V steel [14] very similar to the one used in the present study. A ΔK_{th} value for R=0.90 and ν=0.1Hz is reported to be 3.10 MPa$\sqrt{m}$. ΔK_{th} values for R=0.95 and 0.975 can be estimated by extrapolation of Vosikovsky's analytical expression [14] and are approximately 2.95 and 2.875 MPa$\sqrt{m}$, respectively. Based on these measurements and Eq. 2, the threshold values under ripple-loading conditions of R=0.90, 0.95, and 0.975 are analytically predicted to be 31, 59, and 115 MPa$\sqrt{m}$, respectively. These predicted values are then compared in Table 3 with the experimentally deduced apparent threshold values (from Figs. 1 and 2). As shown in Table 3, under very small ripple-loading of R=0.975, the predicted threshold value is greater than K_{Iscc}. Thus, according to Eq. 3, no RLE is expected as it is in agreement with the experimental results (Fig. 1). For ripple-loading conditions of R=0.90 and 0.95, the predicted threshold values are significantly lower than their experimentally determined counterparts. That is, threshold values based on 4000-hour ripple-load cracking tests are nonconservative. On the other hand, this does not indicate a significant discrepancy between theory and experiment. Rather, as will be shown next, it indicates that the experimental threshold based on a 4000-hr test was marginally too short, as such a duration virtually overlaps the predicted time-to-failure curve developed below in Fig. 5 for R=0.90. (Note that at higher stress-intensity levels, failure times are on occasion as much as 2-3 times greater than prediction.)

The time-to-failure curve can be predicted by numerical integration of Eq. 9, provided the corrosion fatigue crack growth rate curve is established. Again Vosikovsky's crack growth rate data at R=0.90 is used for numerical integration, relative to the identical cantilever bend-bar geometry used in the experimental work. The procedure is quite straight-forward and involves the fitting of power-law equations

TABLE III - PREDICTED AND MEASURED THRESHOLD VALUES (MPa√m)

		5Ni-Cr-Mo-V Steel			4340 Steel
		R=0.90	R=0.95	R=0.975	R=0.90
ΔK_{th}		3.1	2.95	2.875	3.3
$K^{RL}_{max}\|_{tn}$	Predicted	31	59	115	33
	Measured*	44	80	110	33
K_{Iscc}			110		33

* BASED ON 4000-HOUR TESTS.

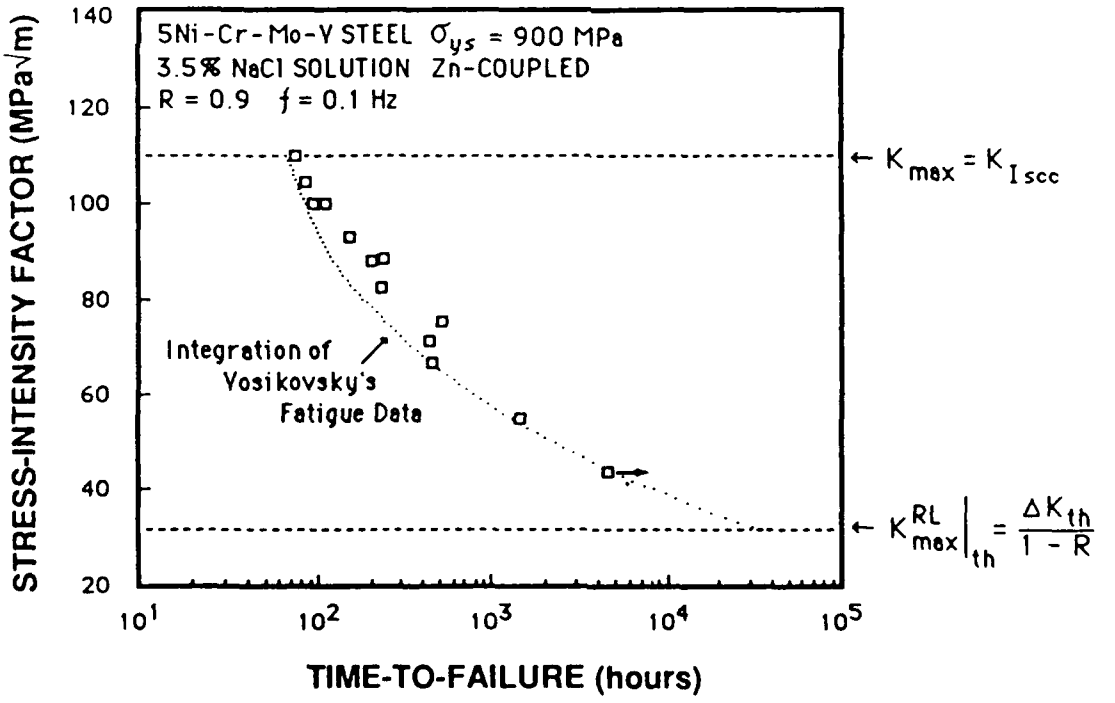

Fig. 5 — Comparison of predicted time-to-failure curve obtained through integration of fatigue data to laboratory data for 5Ni-Cr-Mo-V steel under ripple-loading condition.

in different regions of the crack growth rate data and the subsequent integration using Eq. 9. The predicted time-to-failure curve based on Vosikovsky's data at R=0.90 is presented and compared with the experimental data in Fig. 5. As shown in Fig. 5, excellent agreement between predicted curve and actual experimental data is achieved. This agreement confirms the validity of approaching the ripple-load cracking as an extreme case of corrosion fatigue cracking. Moreover, it is appropriate to observe from Fig. 5 that if experimental determinations of ripple-load threshold were attempted in the vicinity of the predicted value $K^{RL}_{max}|_{th,}$, it is anticipated that the order of 30,000 hrs (~ 3.5 yrs) would be required to provide a failure level in convergence with the predicted value. Thus, a 4000-hr test for ripple-load threshold is inappropriately short in the case of this alloy.

ii) 4340 Steel

To define ΔK_{th}, corrosion fatigue tests were performed in the present study at R=0.90 on 4340 steel specimens in 3.5% NaCl solution. The ΔK_{th} at R=0.90 was found to be 3.3 MPa$\sqrt{m}$. Substituting this threshold value in Eq. 2a, then the threshold level of K --- below which ripple-load cracking will not occur is estimated to be 33 MPa$\sqrt{m}$ which is identical to K_{Iscc} of the 4340 steel. According to the framework predictions of Eq. 3, ripple-load effect will not take place. As it is shown in Fig. 2, this is exactly what happens to 4340 steel under ripple loading (R=0.90) [5]. Thus, the nonsusceptibility of 4340 steel to RLE can be accurately predicted with the proposed framework.

DISCUSSION

It is useful to elaborate somewhat on a number of points related to the predictive methodology offered in this paper. First of all, it is appropriate to ask the question: what material properties tend to promote the high levels of K_{Iscc} and low levels of ΔK_{th} which promote the ripple-load degradation indicated by relations (3) or (4)? In general, higher levels of K_{Iscc} tend to be associated with lower yield strength, higher toughness materials [15]. On the other hand, there is evidence that the lower levels of ΔK_{th} are related to smaller grain size or microstructural mean free path dimension --- and higher yield strength [16, 17]. Thus, interestingly, it would appear that strength level may play competing roles relative to ripple-load degradation.

Secondly, it is useful to focus further on the parameter, $K^{RL}_{max}|_{th}$, and its relation to K_{Iscc} --- since susceptibility or nonsusceptibility of a material to the RLE depends on whether the level of K_{Iscc} exceeds the term, $\Delta K_{th}/(1-R)$, or not (cf. relation (3) or (5)). Even though the numerator (ΔK_{th}) is a parameter that normally decreases with an increase in R, it is clear that the denominator is a quite potent function of R at the high levels of stress ratio concerned with ripple loading ($R \geq 0.90$). Thus if the term, $\Delta K_{th}/(1-R)$, increases significantly with increased R, it may have the potential to rise from levels less than K_{Iscc} to levels in excess. In this way, theoretically at least, a material may be capable of exhibiting both susceptibility and nonsusceptibility to the RLE, depending on the particular value of R. Thus, it appears that susceptibility to RLE is not necessarily a material characteristic.

A few words are also in order regarding the time-to-failure curves. It is significant to note that although the high stress ratio corrosion fatigue data required for the prediction of time-to-failure via Eq. 9 are difficult to obtain from the literature, they may be readily acquired through automated test methods [18]. The predictive framework thus permits the saving of much greater time and expense associated with the direct experimental determination of such time-to-failure curves, reducing the testing time from years to a couple of months --- with much of that time spent determining near-threshold behavior.

The time-to-failure curves, as indicated by Eq. 9, are frequency dependent. Insofar as some alloys exhibit unusual frequency dependency in their corrosion fatigue crack growth behavior, frequency is potentially a significant variable relative to estimates of time-to-failure.

CONCLUSIONS

1. Ripple-loading can, under certain circumstances, significantly reduce time-to-failure and apparent threshold stress intensity for SCC of steels.

2. A predictive framework for the RLE has been developed from concepts and descriptors used in SCC and corrosion-fatigue characterization. Laboratory test results on both the RLE-susceptible and nonsusceptible material successfully confirm the validity of the proposed framework.

3. The critical conditions required for the appearance of RLE have been defined.

4. A mathematical expression has been developed to describe the maximum extent of RLE degradation for specific combinations of material/structure and loading conditions.

5. A more efficient methodology for the establishment of time-to-failure curves for RLE-susceptible materials has been developed.

6. Susceptibility to RLE does not appear to be a material characteristic; rather, if an appropriate value of K_{Iscc} is presumed --- together with a reasonable dependence of ΔK_{th} on R, then a material may theoretically exhibit both susceptibility and nonsusceptibility, depending on the particular level of R.

ACKNOWLEDGMENTS

The support of this work by the Office of Naval Research is gratefully acknowledged.

REFERENCES

1. *Stress-Corrosion Cracking in High Strength Steels and Aluminum and Titanium Alloys*, Edited by B.F. Brown, U.S. Government Printing Office, Washington, D.C. 1972.

2. Hertzberg, R.W., "*Deformation and Fracture Mechanics of Engineering Materials*," Wiley, New York, 1983.

3. Parkins, R.N., and Greenwell,B.S., "The Interface Between Corrosion Fatigue and Stress-Corrosion Cracking," Metal Science, Aug./Sept. 1977, pp. 405-413.

4. Ford, F.P., and Silverman, M., "The Effect of Loading Rate on Environmentally Controlled Cracking of Sensitized 304 Stainless Steel in High Purity Water," Corrosion-NACE, Vol. 36, No. 11,Nov. 1980, pp. 597-603.

5. Crooker, T.W., Hauser II, J.A., and Bayles, R.A., "Ripple-Loading Effects on Stress-Corrosion Cracking in Steels," in *Proceedings of Third International Conference on Environmental Degradation of Engineering Materials - III,* Edited by Louthan, Jr., M.R., McNitt, R.P., and Sisson, Jr., R.D. , The Pennsylvania State University Press, University Park, PA, 1987, p. 521.

6. Mendoza, J. Avila and Sykes, J.M., "The Effect of Low-Frequency Cyclic Stresses on the Initiation of Stress Corrosion Cracks in X60 Line Pipe Steel in Carbonate Solutions," Corrosion Science, Vol. 23, No. 6, 1983, pp. 547-558.

7. Fessler, R.R. and Barlo, T.J., "Threshold-Stress Determination Using Tapered Specimens and Cyclic Stresses," in *Environment-Sensitive Fracture: Evaluation and Comparison of Test Methods, ASTM STP 821*, Edited by Dean, S.W., Pugh, E.N. , and Ugiansky, G.M., ASTM, Philadelphia, 1984, pp. 368-382.

8. Endo, K., and Komai, K., "Effects of Stress Wave Form and Cycle Frequency on Low Cycle Corrosion Fatigue," in *Corrosion Fatigue: Chemistry, Mechanics, and Microstructure, NACE-2*, Edited by Devereax, O.F., McEvily, A.J., and Staehle, R.W., NACE, Houston, 1972, pp. 437-450.

9. Endo, K., and Komai, K., "Influences of Secondary Stress Fluctuations of Small Amplitude on Low-Cycle Corrosion Fatigue," in *Corrosion Fatigue Technology ASTM STP 642*, Edited by Craig, Jr., H. L., Crooker, T.W., and Hoeppner, D.W., ASTM, Philadelphia, 1978, pp. 74-97.

10. Crooker, T.W., and Hauser, II, J.A., "A Literature Review on the Influence of Small-Amplitude Cyclic Loading on Stress-Corrosion Cracking in Alloys," NRL Memorandum Report 5763, Naval Research Laboratory, Washington, D.C., 1986.

11. Judy, R.W., Jr., King, W.E., Jr., Hauser II, J.A., and Crooker, T.W., "Influence of Environmental Variables on the Measurement of Stress-Corrosion Cracking Properties of High-Strength Steels," NRL Memorandum Report 5896, Naval Research Laboratory, Washington, D.C., 1986.

12. Wei, R.P., and Landes, J.D., "Correlation Between Sustained Load and Fatigue Crack Growth in High Strength Steels," Materials Research and Standards, Vol. 9, No. 7, 1969, pp. 25-28.

13. Krausz, A.S., and Krausz, K., "*Fracture Kinetics of Crack Growth*," Kluwer Academic Publishers, Boston, 1988.

14. Vosikovsky, O., "Frequency, Stress Ratio, and Potential Effects on Fatigue Crack Growth on HY130 Steel in Salt Water," J. Testing and Evaluation Vol. 6, No. 3, 1978, pp. 175-182.

15. Sandoz, G., "High Strength Steels," in *Stress Corrosion Cracking in High Strength Steels and Aluminum and Titanium Alloys*, Edited by Brown, B.F., U.S. Government Printing Office, Washington, D.C., 1972, pp. 79-145.

16. Yoder, G.R., Cooley, L.A., and Crooker, T.W., "A Critical Analysis of Grain-Size and Yield-Strength Dependence of Near-Threshold Fatigue Crack Growth in Steels," in *Fracture Mechanics: Fourteenth Symposium --- Vol. 1: Theory and Analysis, ASTM STP 791*, Edited by Lewis, J.C., and Sines, G., ASTM, Philadelphia, 1983, pp. 348-365.

17. Taira, S., Tanaka, K., and Hoshina, M., "Grain Size Effect on Crack Nucleation and Growth in Long-Life Fatigue of Low-Carbon Steel," in *Fatigue Mechanisms, ASTM STP 675*, Edited by J.T. Fong, Philadelphia, 1979, pp. 135-162.

18. Donald, J.K., and Schmidt, D.W., "Computer-Controlled Stress Intensity Gradient Technique for High Rate Fatigue Crack Growth Testing," J. Testing and Evaluation, Vol. 8, No. 1, May 1980, pp. 19-24.